

F.S. Goulding, D.A. Landis and N.W. Madden

Lawrence Berkeley Laboratory
University of California, Berkeley
Berkeley, California 94720 U.S.A.

DISCLAIMER

This report was prepared as an account of work sponsored by an agency of the United States Government. Neither the United States Government nor any agency thereof, nor any of their employees, makes any warranty, express or implied, or assumes any legal liability or responsibility for the accuracy, completeness, or usefulness of any information, apparatus, product, or process disclosed, or represents that its use would not infringe privately owned rights. Reference herein to any specific commercial product, process, or service by trade name, trademark, manufacturer, or otherwise, does not necessarily constitute or imply its endorsement, recommendation, or favoring by the United States Government or any agency thereof. The views and opinions of authors expressed herein do not necessarily state or reflect those of the United States Government or any agency thereof.

ABSTRACT

The paper describes the philosophy behind the design of a pulse processing system used in a semiconductor detector x-ray spectrometer to be used for plasma diagnostics at the Princeton TFTR facility. This application presents the unusual problems of very high counting rates and a high-energy neutron background while still requiring excellent resolution. To meet these requirements three specific new advances are included in the design:

- (i) A symmetrical triangular pulse shape is employed in the main pulse-processing channel. A new simple method of generating a close approximation to the symmetrical triangle has been developed.
- (ii) To cope with the very wide dynamic range of signals while maintaining a constant fast resolving time, approximately symmetrical triangular pulse shaping is also used in the fast pulse pile-up inspection channel.
- (iii) The demand for high throughput has resulted in a re-examination of the operation of pile-up rejectors and pulse stretchers. As a result a technique has been developed that, for a given total pulse shaping time, permits approximately a 40% increase in throughput in the system.

Performance results obtained using the new techniques are presented.

1. INTRODUCTION

High temperature plasmas such as that to be produced in the Princeton Tokamak Fusion Test Reactor (TFTR) emit considerable black body radiation in the x-ray energy range up to several tens of kilovolts. In experiments with the reactor, measurement of the x-ray flux will be an important tool in measuring the plasma temperature and in detecting the presence of impurities by observation of their characteristic x-ray lines. Furthermore, such experiments must measure the spatial and temporal variations of these parameters.

To observe the spatial distribution of x-rays, long collimators are provided to permit a total of 36 x-ray detectors to be exposed to different regions in the plasma. Six of the detectors are germanium to provide good absorption characteristics for x-rays of energies up to 50 keV; the remainder are silicon to adequately cover the lower x-ray energy range. Since temporal variations during the plasma pulse must be observed on a millisecond time scale, the solid angle of the detectors observing the plasma must be large enough to give counting rates adequate for statistically meaningful spectra to be accumulated on a time scale of a few milliseconds. The combination of very high counting rates and the excellent energy resolution required to observe and separate impurity spectral lines presents very difficult design problems in semiconductor detector spectrometers. Moreover, we

note at the outset that the final usefulness of the technique demands that a high rate of analyzable pulses be passed by the signal processing system—rejection of events must be minimized and a high throughput is essential.

Since the whole purpose of TFTR is to produce thermonuclear reactions, significant production of 14 MeV neutrons must be anticipated. The estimated maximum flux of such neutrons through the detectors is ~ 5000/sec; they interact by colliding with silicon (or germanium) nuclei resulting in signals ranging up to a few MeV. The signal processing system must cope with these large signals and recover very quickly to process the x-ray signals in the energy range from 1 keV to 50 keV.

Another significant aspect of work at TFTR is the pulsing of very intense magnetic and electric fields in near proximity to the sensitive detection systems. This demands extreme care in the grounding and in the design of the pulse processing system. The spectrometer system designed for this application consists of modules of six detectors (one germanium and five silicon) mounted in a close-packed circular cluster. Associated with each group of 6 detectors is the cryostat, preamplifier and electronic distribution box. Figure 1 shows a photograph of a six-detector system. Electrical connections from this unit are taken via a copper conduit to the instrument racks located about 20 feet away from the detector system. Great care is taken to maintain a single-point ground for each detector set. The instrument racks contain power supplies, pulse processing electronics and A.D.C.

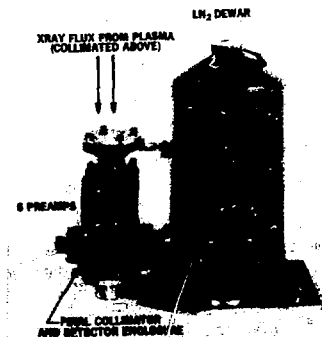


Fig. 1. Photograph of plasma diagnostics x-ray system containing five silicon and one germanium detector.

6248

Digital outputs from the ADC's are fed via light couplers to the computer room, thereby providing good ground isolation for the sensitive detector and analog circuits. Magnetic shielding is provided surrounding the whole front end system. This requirement and the need for close packing of units resulted in the very compact design of the system.

The main purpose of this paper is to discuss the philosophy of the design of the pulse processing electronics used in this system. However, a key part of the overall system is the front-end including the detector, FET and preamplifier, and a few words will be devoted here to these items. The detectors used here have active regions 4.3 mm in diameter and are 3.3 mm thick. A cross-sectional view of one detector is shown in Figure 2. As indicated earlier, one detector in each system is germanium; the remaining five are silicon. The x-rays are collimated to a region 3.3 mm in diameter in the center of the detector; this is done to avoid the detector background that would occur if substantial charge collection occurred in surface layers. The FETs used in these systems are selected units of the 2N416 general class and they are decanned and mounted in a special low-loss package. Transistor reset is employed to restore charge on the feedback capacitor; this is preferred over pulsed-light reset in this application because the inter-channel feedthrough produced by resets is very much improved using this method. Pulsed-light feedback suffers from serious interchannel feedthrough in multi-detector systems such as this. Figure 3a shows a photograph of the small package that provides an integrated mount for detector, FET and reset transistor. Blown up views of the component parts are included. Fig. 3b shows the complete assembly of six front ends included in the detector enclosure of Fig. 1.

The preamplifier is shown in block form in Fig. 4. The particular features of the preamplifier include:

- (i) In addition to the signal output, a ground point obtained from the vicinity of the signal output driver is brought out as an output signal. These two lines are used as balanced inputs to the pulse processor; this feature is provided to make the system less sensitive to electrical noise.

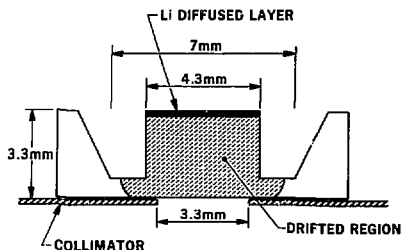


Fig. 2. Cross-sectional view of one of the silicon detectors.

- (ii) The input charge-sensitive loop is designed to provide a fast risetime (~ 20 ns) so that signal integration in the fast processing channel can be determined by a deliberate integrator included in the fast signal processor.
- (iii) Test signals are injected through the detector capacitance. These signals are produced by an FET chopper included in the preamplifier unit. A single line input to this chopper provides both the dc reference level to the chopper and a biphasic signal to initiate the chopping. This technique completely eliminates the possibility of injection of electrical noise into the front end via test pulser lines and provides a reference pulse of high accuracy (~ 1 in 1000) unaffected by cable length.

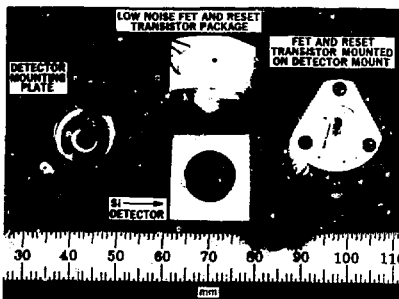


Fig. 3a. Photograph showing the detector/FET module and its parts.

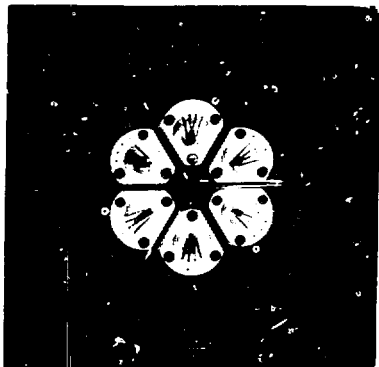


Fig. 3b. Photograph showing six modules mounted in detector enclosure.

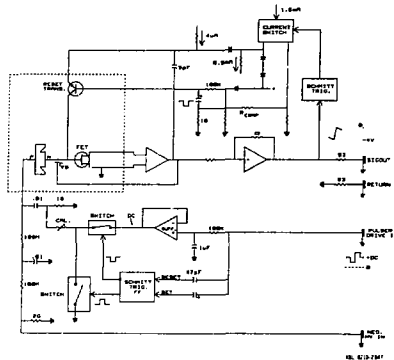


Fig. 4. Block diagram of the preamplifier.

2. OPTIMIZING PULSE SHAPE

Much of the literature dealing with optimizing pulse shape to obtain the best energy resolution in spectroscopy systems focuses on cases where parallel (step) and series (δ) noise are present and where choice of the time scale (or measurement time) can be made to equalize these two terms. It is well known that the cusp-shaped waveform is ideal when these constraints are applicable. With presently available FETs, and using small silicon x-ray detectors, the optimum shaping time in these circumstances may well be in the 100 μ s range. In applications where high counting rates are essential, such as the one dealt with in this paper, pulse shaping times in the 100 μ s range are unacceptable, and we are forced to use relatively short times. Under these circumstances the dominant noise source is series (δ) noise caused primarily by the fluctuations in the channel current in the FET.

Therefore, in our application, the problem of optimizing pulse shape is simplified to that of choosing a pulse shape that, for a given total duration gives the best signal/noise ratio when only series (δ) noise is present. We note that the $1/f$ noise component should contribute little in these circumstances and is rather insensitive to the particular choice of pulse shape. The problem is best dealt with analytically using the time-domain method³, and it has been shown⁴ that the symmetrical triangular pulse shape is the best in this situation. This result follows directly from the fact that the weighting function of a time invariant pulse shape for delta noise is given by

$$\overline{N_d^2} = \int_0^{\tau} \{f'(t)\}^2 dt \quad (1)$$

here $f(t)$ is the step response of the system and $f'(t)$ is its differential. It is easy to see that N_d^2 assumes a minimum value when the absolute value of $f'(t)$ remains constant during the entire pulse width; the symmetrical triangular pulse shape achieves

this. If $f'(t)$ is smaller at any time during the pulse, it must inevitably be larger at another time if the same amplitude and total pulse width is to result; since N_d^2 involves integration of $\{f'(t)\}^2$ over the entire pulse width, an increase in N_d^2 must result. Derivation of a symmetrical triangular pulse shape has presented a generation of designers with an insurmountable problem. It has long been recognized that proper integration of a symmetrical biphasic delay line pulse achieves the desired result, but delay lines are bulky, are not easily varied in their time scale, and cause severe sensitivity of gain to temperature variations. Therefore, they are not considered ideal circuit elements for the main channel of pulse processors. To provide a close approximation to the required symmetrical triangle, the scheme illustrated in Fig. 5 was devised. It involves weighted mixing of the outputs of stages that are already present in most shaping amplifiers producing Gaussian pulse shapes; therefore, it uses convenient active integrators whose behavior is suitable for stable amplifiers (unlike delay lines). In this amplifier, the early differentiator is followed by the first active integrator stage, which inverts, while the last two active integrators are of the non inverting type first used in nuclear pulse amplifiers by Fairstein. Analytically the stages are analogs of each

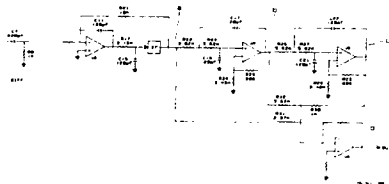
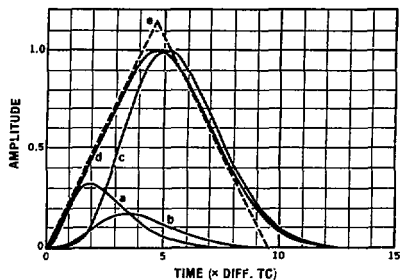


Fig. 5. Block diagram of the symmetrical triangle pulse shaper.

other, all having their poles about 27.3° off the real axis. Waveforms from the outputs of the first, second and third stages are mixed in the ratio of 0.324:0.168:1 respectively to produce the approximately symmetrical triangular output waveform. Figure 6 shows the three component waveforms (a, b, c) with amplitudes corresponding to the weighting used in the amplifier together with the resulting almost triangular wave, (d) produced by adding these three components and normalizing to unity amplitude. A true symmetrical triangle (e) closely matching the sides of the waveform (d) is also shown. The waveforms shown in Fig. 6 are calculated; experimentally observed waveforms are essentially identical to these.

We observe that the output waveform departs from the true symmetrical triangle in two significant respects:

- (i) The peak is rounded; this feature increases the parallel (step) noise slightly but is also a necessary feature for good operation of the pulse stretcher used at the output of the system. Since the parallel noise is negligible in this application virtually no loss of performance results.



LBL 6210-2874

Fig. 6. Waveform used to construct the symmetrical triangle:

- a) First stage output
- b) Second stage output
- c) Third stage output
- d) Sum of three components (normalized to unity amplitude)
- e) True symmetrical triangle for comparison with d).

- (ii) A slightly rounded tail occurs on the output pulse. This is unfortunate since it increases pulse pile-up effects a little but it is unavoidable using passive (i.e., time-invariant) networks. Choice of the active integrator and differentiator stages is based on minimizing this effect.

A good basis for comparison of the noise performance of a system producing the waveform (d) for a step function input, is provided by comparing it with the performance of a system producing the quasi-Gaussian waveform (c) which is typical of many modern spectroscopy systems. Calculation shows that an improvement of about 8% in series (Δ) noise resolution would be expected and experimental work confirms this. It is interesting to study the waveforms of Fig. 6 and to observe the reason for the improvement, remembering that the integral of the (slope)² is the important factor in series (Δ) noise. Obviously very little difference exists between waveforms (c) and (d) on the falling part of the waveforms, but the rising slope of waveform (d) is constant and much smaller than the steepest part of the rising slope of waveform (c). This avoidance of excess slope is the fundamental reason for the improved Δ noise achieved by using waveform (d). It is also clear that the increased "area" of (d) compared with (c) will slightly worsen parallel (step) noise which depends on the integral of the square of the step function response. The effect on parallel noise is only about 5%; since parallel noise is negligible in all high rate systems, this has virtually no practical effect on performance.

3. SHAPING IN FAST CHANNEL

All modern spectrometer pulse processors use a method for preventing the analysis of pulses whose amplitude is subject to interference of other signals in close time proximity. Generally soaking this function is achieved by a "pile-up rejector" containing three elements:

- (a) A gate at the output of the slow pulse processing channel.
- (b) A parallel fast inspection channel where signals are differentiated to form narrow pulses. A fast discriminator is used to detect such signals and produce logic signals.
- (c) A pile-up detector which examines the output signals from the fast discriminator, and, by measuring the time intervals between these signals, senses where pile-up effects in the slow channel may distort the signal amplitude in that channel. When such a pile-up condition is not present, the pile-up detector produces an output that opens the signal gate in the slow channel. If a pile-up is sensed, the slow signal is inhibited by the gate.

As we will see in the next section, a detailed examination of this process shows that substantial improvements can be made in the common methods of implementing these functions and that these methods reject more pulses than is absolutely required. However, in this section we focus attention on another aspect of this pile-up rejection technique which is particularly important in the plasma diagnostics application.

As indicated earlier, narrow pulses are formed in the "inspection" channel, and the output width of the fast discriminator corresponds to the time that a narrow signal pulse amplitude exceeds the discriminator threshold level. If two signal pulses occur within this "resolving time", the inspection channel cannot recognize them as separate signals, and the slow signal channel is not closed. In the slow processing channel this results in a small number of output pulses whose amplitude is the sum of two (or more) separate signals and the output spectrum contains "sum" peaks. These will be illustrated in the final section of the paper. It is easy to see that this process will distort the thermal black body spectrum seen from hot plasma discharges because some counts that should appear in the intense low energy part of the spectrum are shifted into the weak high energy part of the spectrum. Such distortion of the black body radiation spectrum will affect the measurement of the plasma temperature. If the resolving time of the fast channel is reasonably well known, an approximate correction can be applied to the continuum spectrum for this type of pulse pile-up.

Unfortunately, existing spectrometers fall far short of meeting the criteria of providing a well-determined resolving time in the fast inspection channel. Typically these instruments use (accidental) integration (mostly in the preamplifier) and single delay line or simple RC pulse shaping. With such an arrangement the long exponential tail on the back edge of the signal waveform, as shown in Fig. 7a, causes the resolving time to be very dependent on pulse amplitude and makes the resolving time difficult to determine in cases where a wide and unknown dynamic range of pulse amplitudes is to be measured. Furthermore, most existing systems do not permit choice of the integrator and (delay-line) differentiator to optimize the signal/noise of the fast channel, so the fast discriminator level must be set high to reduce noise triggering.

To overcome these problems the pulse shaper shown in the block schematic Fig. 9 was devised. Here a

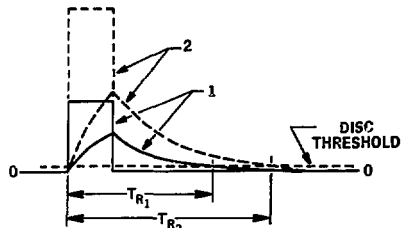
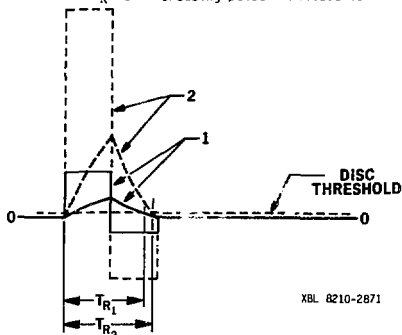


Fig. 7a. Fast channel pulse shapes in a conventional system. The widening of the resolving time T_R for increasing pulse amplitude is shown.



XBL 8210-2871

Fig. 7b. Fast channel pulse shapes in new system. The final outputs (1) and (2) are produced by RC integration of the asymmetrical bipolar delay line waveform.

known RC integrator is combined with an asymmetrical bipolar delay line pulse shaper to produce an output waveform (see Fig. 7b) that returns precisely to the baseline at a time equal to the total bipolar pulse width. This condition can be satisfied in many ways but a convenient one is to choose an RC integrator time constant equal to the delay line length (i.e., $1/2$ the total pulse width) and to make the amplitude of the second half of the bipolar pulse $1/e$ times that of the first half. It is simple to show that this produces the desired output pulse; it also results in a waveform that is a reasonably close approximation to a symmetrical triangle which is known to give the best signal/noise ratio where series (Δ) noise is dominant (as it always is in the fast channel) and where a maximum pulse width constraint applies.

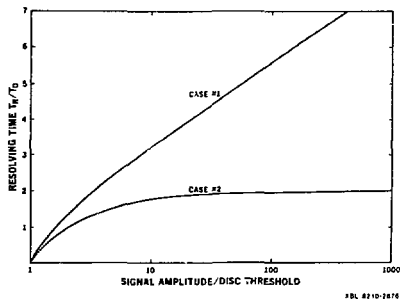
The behavior of the resolving time of the two types of systems is shown in Fig. 7. It is clear that the resolving time (T_{R1} and T_{R2}) is much less sensitive to amplitude variations in the case of Fig. 7b than in that of Fig. 7a. For the special case of Fig. 7a where the RC integration time T_0 is equal to the delay-line shaped pulse width we have:

$$T_R = T_0 \ln(e/x - e^{-1}) \quad (2)$$

On the other hand, the case of Fig. 7b where the amplitude of the second half of the biphasic delay line pulse is $1/e$ of that of the first half gives:

$$T_R = T_0 \ln\{e\{e - x(e-1)\}/[1 + x(e-1)]\} \quad (3)$$

In these equations, x is the ratio of the value of the discriminator threshold to the peak output signal amplitude. These relationships are illustrated graphically in Fig. 8 which clearly shows the improved behavior of the resolving time in the second case as the amplitude varies.



PBL 8210-2876

Fig. 8. Behavior of the resolving time of a fast channel as a function of pulse amplitude. Case 1 is for a conventional system while Case 2 is for the new system.

The operation of the fast pulse shaper shown in Fig. 9 is as follows:

- (i) The first amplifier stage performs a subtraction operation between the input step function (a) and a delayed version of the input. The resulting output (b) is a single phase rectangular pulse.
- (ii) The second stage performs a subtraction between the waveform (b) and a delayed (adjustable amplitude) version of (b) which is delayed by its width. The result is waveform (c).
- (iii) The third stage provides an RC integrator whose time constant is equal to the width of pulse (b). The result is waveform (d) which closely approximates a symmetrical triangle.

The first two stages and a third one that provides bias for the first two are standard ECL line receivers all contained in a single package. Discrete transistors are used in the integrator stage.

4. THROUGHPUT CONSIDERATIONS/PILE-UP REJECTION

The requirement to achieve the maximum possible throughput in this system led to a reconsideration of the operation of existing pile-up rejection systems and the development of a new scheme that gives a considerable improvement in throughput.

$$T_{D2} = T_1 + T_2 = T_W \quad (5)$$

where T_W = total pulse width.

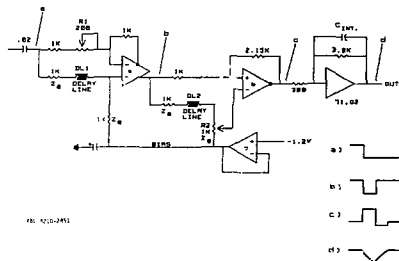


Fig. 9. Block diagram of the new fast channel pulse shaper.

We will illustrate some of the considerations by using Fig. 10a which shows an initial signal (0) followed by signals at four selected times later. To simplify the diagram, an asymmetrical triangular waveform is shown with a rise time of T_1 and a slower fall time of T_2 . The four cases of second pulses can be described as follows:

Case 1. The start of this pulse occurs during the rise of signal 0. It is clear that the peak amplitudes of pulse 0 and 1 are both affected by the pulse interference so both signals must be rejected.

Case 2. The start of this pulse is later than the peak of pulse 0 but the peak of pulse 2 precedes the end of pulse 0 and its peak amplitude will be subject to interference. Therefore, in this case it is mandatory that the second pulse (?) be rejected while the first pulse (0) is accepted.

Case 3. This case is similar to case 2 but the peak of pulse 3 occurs after pulse 0 is completely finished. An ideal pile-up rejector would allow processing of both pulse 0 and pulse 3 but existing systems do not permit this. This situation generally results from the fact that the pulse stretcher circuit waits until the tail of the first pulse reaches a low threshold level before permitting the stretching of a normal pulse.

Case 4. Here the whole signal 4 follows the end of pulse 0 and both signals can be processed.

From this analysis it is clear that any improvement in throughput compared with existing systems depends on devising a pile-up rejector system that accepts pulses in category 3. The effect of such acceptance is substantial. The normal pile-up system rejects both pulses corresponding to case 1 and rejects the second one corresponding to cases 2 and 3. This results in an effective dead time for loss calculations equal to T_{D1} where:

$$T_{D1} = 2T_1 + T_2 \quad (4)$$

On the other hand, a pile-up rejector that permits processing of pulses in category 3 imposes an effective dead time given by:

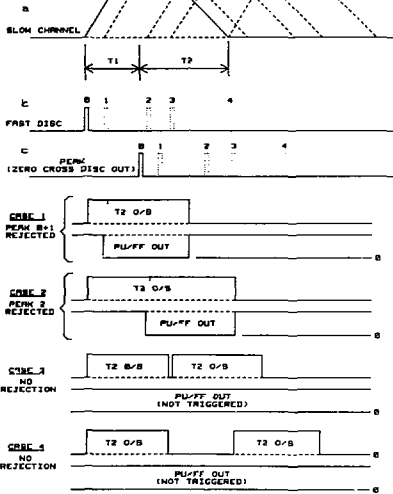


Fig. 10. Illustration of the various pile-up conditions. The text provides description of these cases.

For the special case of a symmetrical triangular shape where $T_1 = T_2$, we have $T_{D1} = 1.5 T_W$ while $T_{D2} = T_W$. Therefore a 50% improvement in the maximum throughput results. The actual design discussed in this paper is best characterized by assuming $T_1 = 4\mu s$ and $T_2 = 5\mu s$ so $T_{D2} = 9\mu s$ while the value of T_{D1} (i.e. rejection of pulses in class 3) will be $13\mu s$. A graphic illustration of the performance in the two cases is given in Fig. 11 where throughput curves are presented as a function of input counting rate for the two cases. Experimental points are also given in this graph. We see that the peak output rate is increased by about 35% by using the improved pile-up rejector system.

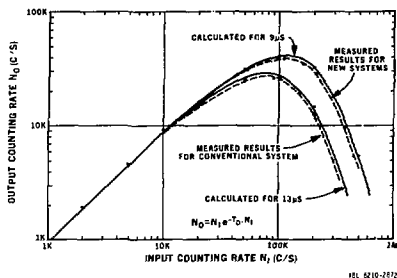


Fig. 11. A plot of output versus input counting rate for a system using conventional pile-up rejection and for the new system. A 35% improvement in peak throughput is observed.

The overall block diagram given in Fig. 12 will be used in this discussion of the operation of the pile-up rejection logic. The condition for acceptance of a pulse peak for processing can simply be stated (see Fig. 10) as requiring that no earlier pulse peak occurs in the time T_2 (i.e. the decay time) preceding the peak in question. For example, pulse 3 in Fig. 10 just meets this condition.

In Fig. 12, normal processing (i.e. no pile up) of a signal pulse involves the "Track and Hold" circuit output following the final symmetrical triangular

signal waveform until the "Stretch One-Shot" disconnects the "hold" capacitor C_H from the signal. The 2 μs "Stretch One-Shot" is triggered by a peak sensing circuit consisting of the differentiator ($C_2 R_2$) and the Zero Crossing Discriminator; these circuits are designed to sense precisely the peak of the final symmetrical triangle so that the hold capacitor C_H holds the peak voltage for 2 μs . A linear gate on the output of the "Track and Hold" circuit produces a 0.75 μs wide output pulse whose start is delayed by 0.5 μs after the peak of the symmetrical triangle.

Rejection of pulses subject to pile up is accomplished by using the pile-up waveform generated by the "Pile-up FF" to close the input gate on the "Stretch One-Shot". The "Pile-up FF" is held in its reset condition by the output line of the "T2 One-Shot" until this is triggered by the back edge of a pulse from the fast discriminator. The "T2 One-Shot" is an extending type of one-shot that generates a positive output level for a time T_2 (equal to the trailing part of the signal pulses in Fig. 10) after each fast discriminator pulse. This enables the "Pile-up FF" to be set by its clock input if a further fast discriminator arrives while the reset input of the "Pile-up FF" is high.

In the bottom part of Fig. 10, the behavior of the T2 one-shot and pile-up flip-flop outputs is shown for each of the four cases illustrated in Fig. 10a. Figure 10b shows the fast discriminator outputs for the four cases and Fig. 10c shows the output pulses from the peak detector circuit. The behavior shown in Fig. 10 is largely self-explanatory; we note that case 3 represents the marginal case where the second event is just accepted; if signal pulse 3 were slightly delayed, its acceptance would clearly occur.

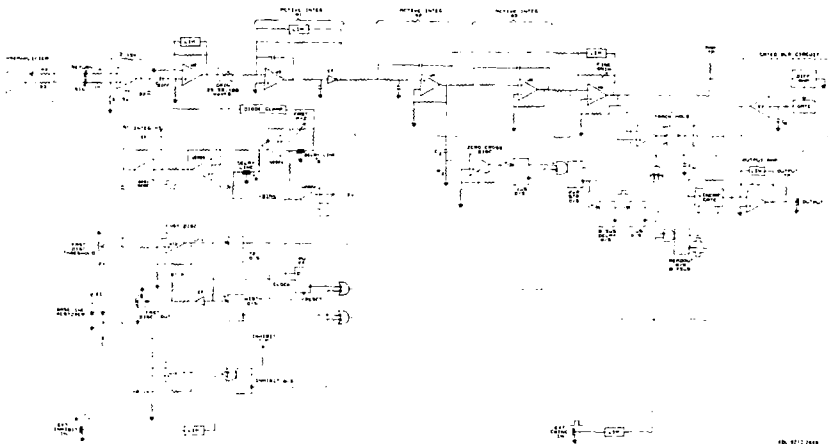


Fig. 12. Block diagram of the whole pulse processor.

5. OVERALL SYSTEM

The principal new features of the system have already been discussed but a few remarks should be directed to certain parts of the overall system shown in Fig. 12 because these also contribute significantly to the overall performance. We note that feedback limiters are used on two of the amplifying stages of the main processor, on one of the active integrator stages and on the final output stage. These limiters play an important role in minimizing the system recovery time following the large overload pulses produced by fast neutrons in the detectors. We also note the use of a gated base line restorer that uses the "Width O/S" output waveform as the gating waveform. This reduces the slight offset normally produced in restorers at high rates to a negligible amount.

6. EXPERIMENTAL RESULTS

A. Energy Resolution

A total of 12 individual spectrometers (i.e., two 6-channel units) using these principles has been produced at the present time. As indicated in sections 2 and 4, the pulse width chosen for this application corresponds to a peaking time of 4 μ s for the symmetrical triangle. The average value of the FWHM resolution measured on the 5.9 keV Mn K-x-ray is 225 eV with a spread between units of about 10 eV. This is consistent with a measured electronic FWHM resolution of 189 eV. We note that this would correspond to 95 eV FWHM if the peaking time was changed to 16 μ s giving a total pulse width of about 36 μ s and a peak throughput of just over 10,000 counts per second.

A useful relationship for calculating the energy resolution (Δ noise only) of a silicon detector spectrometer using a simple RC integrator/differentiator is:

$$E_{FWHM} = 215 C / g \tau_0 \text{ eV} \quad (6)$$

where C is the total input capacity in pF
 g is the FET transconductance in mA/V
 τ_0 is the time constant (peaking time) of an RC/RC integrator/differentiator pulse shaper.

For our waveform (almost symmetrical triangle) peaking at the same time as the RC/RC shaper we have

$$E_{FWHM} = 223 C / g \tau_0 \text{ eV} \quad (7)$$

If we assume that C = 5 pF, g = 9 mA/V and $\tau_0 = 4 \mu$ s, we obtain an energy resolution of 186 eV in good agreement with the experimentally measured resolution of 189 eV. The values of C, g, and τ_0 are consistent with those expected in the system. Therefore, it is apparent that no additional significant noise sources exist.

B. Resolving Time of Fast Channel

(i) Sum peaks

For the plasma diagnostics system, 3 fast shaping boards using delay lines 60 ns, 200 ns and 450 ns long are provided; depending on the specific channel and its anticipated counting rate, the appropriate board may be used. Use of a short shaping time reduces sum peaks in a spectrum but, since the noise amplitude varies as $1/\tau_m$

where τ_m is the shaping time, the fast channel is more noisy when short shaping times are used. To avoid excessive noise triggering, the fast discriminator threshold must be raised, so pile-up of low-amplitude pulses is not sensed by the inspection channel. Furthermore, since the T2 One-Shot (Fig. 12) is not triggered, the zero-cross discriminator that performs peak sensing is not enabled. Therefore, the fast discriminator threshold also imposes a lower level threshold on all processed signals.

Measurement of the rates of sum peaks when counting at high rates can be used to determine an effective fast channel resolving time. We have carried out such measurements both with purely random pulses and by measuring pile-up effects when a regular (relatively low-rate) pulser is mixed with a random source. Figure 13 shows an example of these results using the 200 ns shaping board (this gives a maximum resolving time of 400 ns). The results shown in Fig. 13 were all acquired using an ^{59}Fe source at an input counting rate of 442 kHz, and successive pictures in the sequence show expansion of the vertical display scale. The following features should be noted:

- ... Despite the high counting rate, the general background is very low, illustrating the total lack of general pile-up events. The upper picture (c) vertical full scale is 80 counts while the lower one (a) is 25,000 counts.
- ... We comfortably observe sum peaks as far out as quadruple events within the resolving time of the fast channel. We also note that the sum peaks consist of combinations of coincident K_{α} and K_{β} x-ray events so more than the $K_{\alpha} + K_{\beta}$ peaks seen in the singles spectrum are observed.
- ... The fast channel resolving time calculated from these spectra is 320 ns. This is substantially shorter than the expected maximum value of 400 ns but is close to the value expected based on Fig. 8 for a ratio of signal amplitude/disc threshold of 5:1.

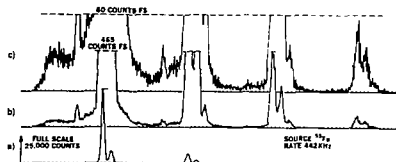


Fig. 13. Illustration of sum peaks produced by pile-up within the resolving time of the fast channel. The spectra are identical, but the vertical full-scale is 25,000 counts (a), 465 counts (b), 80 counts (c).

(ii) Fast Discriminator Threshold

We can use the relationship of Eqn. 7 to predict the noise in the fast channel since the pulse shaping in this channel also approximates a symmetrical triangle. Using the 200 ns delay line, the predicted FWHM noise is approximately 850 eV. A good rule of thumb is that noise counts become negligible when the fast discrimination level is set to 4.5 times the RMS noise value. This means that the threshold can be set to about 1.6 keV when using the 200 ns delay line shaper. The equivalent value for the 60 ns line is 3 keV and it is approximately 1 keV for the 450 ns line.

The effect of the fast discriminator threshold is not to cause an abrupt cut-off in signals processed by the slow channel, but because noise modulates the signals feeding the fast discriminator, a slow roll-off of accepted counts occurs as the signal amplitude is reduced. This is illustrated in Fig. 14. For this figure the fast discriminator was set to a level at which noise triggers it at a rate of 100 c/s. A calibrated pulser was injected into the system and fixed-time counts were taken with the pulser set to different amplitudes. An ^{55}Fe source was counted at the same time. The roll-off in efficiency at low energies is clearly observed and it is consistent with the noise behavior calculated in the previous paragraph for the 200 ns delay line shaper. A slight discrepancy in the roll-off may be ascribed to the pulser rise-time being longer than that of detector signals.

this test is thought to give a reasonable approximation to the 5 kHz of neutron events to be encountered in the x-ray diagnostics application.

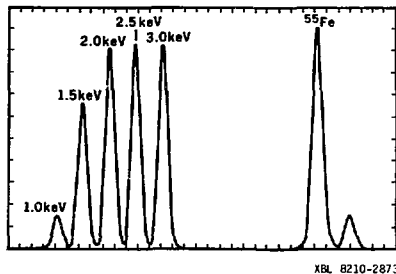


Fig. 14. Illustration of loss of efficiency at low-energies due to the setting of the fast discriminator threshold level.

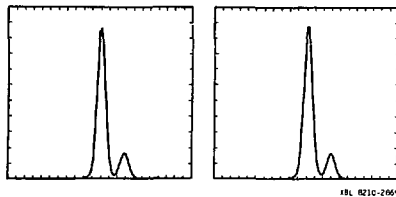


Fig. 15. Illustration of the effect of overloads on resolution. The left-hand curve shows an ^{55}Fe spectrum accumulated with an input rate of 100 kHz, while the right-hand one represents the same conditions except for the simultaneous presence of 20 kHz of $^{90}\text{Sr} + ^{90}\text{Y}$ β -particles (end point energy = 2.28 MeV).

C. Throughput

The experimentally measured throughput results shown in Fig. 11 agree very well with the theoretical curves for the 9 μs total pulse width. The slight discrepancy indicates that the effective pulse width is slightly over 9 μs .

D. Overload Behavior

As indicated in the first part of the paper, this system must provide excellent resolution for low-energy x-rays at the same time as being subjected to large signals (up to a few MeV) produced by fast neutrons in the detectors. A relatively high rate (~ 5 kHz) of such signals is anticipated under some operating conditions of TFTR.

A completely valid test of the performance under these conditions is difficult to devise and several have been used in evaluating the performance. Figure 15 presents an example of one test. In this figure, the left-hand spectrum shows the Mn Ka and Ka lines produced by an ^{55}Fe source. The input rate (i.e., fast discriminator triggering) was 100 kHz. The right-hand figure shows performance under the same conditions except that a ^{90}Sr source was counted at the same time, producing a counting rate of an additional 20 kHz in the detector. As can be seen, virtually no deterioration in the x-ray resolution is observed. While the β spectrum of ^{90}Sr (^{90}Y) does not duplicate the fast neutron knock-on spectrum in the detector, it does contain events in the correct energy range and the high rate used in

ACKNOWLEDGMENTS

We thank the diagnostics group at the Princeton TFTR for drawing our attention to the special problems involved in the application of semiconductor detector spectrometers to x-ray plasma diagnostics. Thanks are particularly due to K. Young, K. Hill, and S. von Goeler. The main funding for the project was supplied by the TFTR program. Much of the work resulted from work supported by the Director's Office of Energy Research, Office of Health and Environmental Research, U.S. Department of Energy under Contract No. DE-AC03-76SF0098.

We also wish to thank D. Malone, J. Walton, Y. Wong, A. Jue and E. Converse for fabrication of the detector mechanical parts and electronics used in this work. A special note of thanks must go to C. Cork for his patience and skills in the fabrication of the low-noise front ends. We appreciate the effort of C. Quigley and V. Donelson in the preparation of the manuscript.

REFERENCES

1. F.S. Goulding, J.M. Jaklevic, B.V. Jarrett and D.A. Landis, Detector Background and Sensitivity, Advances in X-Ray Analysis, Vol. 15, 470 (Denver Conference, 1971).
2. D. Landis, C. Cork, N.W. Madden, F.S. Goulding, Transistor Reset Preamplifier for High Rate High Resolution Spectroscopy, IEEE Trans. Nucl. Sci., NS-29, No. 1, 619 (1982).
3. F.S. Goulding, Pulse Shaping in Nuclear Amplifiers: A Physical Approach to Noise Analysis, Nucl. Inst. and Methods 100, 493 (1972).
4. F.S. Goulding, D.A. Landis, Signal Processing for Semiconductor Detectors, (IEEE Nucl. Sci. Symp. Short Course) IEEE Trans. on Nucl. Sci., NS-29, No. 3, 1125 (1982).